Roles of density-dependent growth and life history evolution in accounting for fisheries-induced trait changes

Anne Maria Eikeset[a,b,c,d,e,f,1], Erin S. Dunlop[c,g,h,i,j], Mikko Heino[c,h,i,j], Geir Storvik[k], Nils C. Stenseth[a,b,1], and Ulf Dieckmann[c]

[a]Department of Biology, University of Oslo, N-0316 Oslo, Norway; [b]Centre for Ecological and Evolutionary Synthesis (CEES), University of Oslo, N-0316 Oslo, Norway; [c]Evolution and Ecology Program, International Institute for Applied Systems Analysis, A-2361 Laxenburg, Austria; [d]Center for BioComplexity, Princeton University, Princeton, NJ 08544; [e]Princeton Environmental Institute, Princeton University, Princeton, NJ 08544; [f]Department of Ecology and Evolutionary Biology, Princeton University, Princeton, NJ 08544; [g]Aquatic Research and Monitoring Section, Ontario Ministry of Natural Resources and Forestry, Peterborough, ON, Canada K9L 0G2; [h]Institute of Marine Research, N-5817 Bergen, Norway; [i]Department of Biology, University of Bergen, N-5020 Bergen, Norway; [j]Hjort Centre for Marine Ecosystem Dynamics, University of Bergen, N-5020 Bergen, Norway; and [k]Statistics Division, Department of Mathematics, University of Oslo, N-0316 Oslo, Norway

Contributed by Nils C. Stenseth, November 4, 2016 (sent for review December 15, 2015; reviewed by Andrea Belgrano and Tomas O Höök)

The relative roles of density dependence and life history evolution in contributing to rapid fisheries-induced trait changes remain debated. In the 1930s, northeast Arctic cod (*Gadus morhua*), currently the world's largest cod stock, experienced a shift from a traditional spawning-ground fishery to an industrial trawl fishery with elevated exploitation in the stock's feeding grounds. Since then, age and length at maturation have declined dramatically, a trend paralleled in other exploited stocks worldwide. These trends can be explained by demographic truncation of the population's age structure, phenotypic plasticity in maturation arising through density-dependent growth, fisheries-induced evolution favoring faster-growing or earlier-maturing fish, or a combination of these processes. Here, we use a multitrait eco-evolutionary model to assess the capacity of these processes to reproduce 74 y of historical data on age and length at maturation in northeast Arctic cod, while mimicking the stock's historical harvesting regime. Our results show that model predictions critically depend on the assumed density dependence of growth: when this is weak, life history evolution might be necessary to prevent stock collapse, whereas when a stronger density dependence estimated from recent data is used, the role of evolution in explaining fisheries-induced trait changes is diminished. Our integrative analysis of density-dependent growth, multitrait evolution, and stock-specific time series data underscores the importance of jointly considering evolutionary and ecological processes, enabling a more comprehensive perspective on empirically observed stock dynamics than previous studies could provide.

phenotypic plasticity | eco-evolutionary dynamics | management | genetic adaptation | genetic variance

Harvesting is usually selective, differentially targeting and removing members of a population based on their phenotypic attributes (1, 2). Such selective harvesting induces a genetic response in life history traits when it renders some genotypes more likely than others to survive and reproduce (3, 4). Even nonselective harvesting can induce evolutionary change, through the effects of elevated mortality on the differential survival and reproduction of individuals with specific genetic attributes (5). During the last decade, progress has been made in identifying evolutionary responses to harvest in the wild (6–8), as improved statistical methods for analyzing field data have become available (9, 10). Although trends in life history traits have repeatedly been found to be indicative of genetic adaptations to intense harvest pressures, their concomitance with phenotypically plastic responses to changing environmental conditions often complicates the identification of genetic changes (3, 4, 11–14). An important type of phenotypic plasticity affects growth rates and maturation schedules and is known as the compensatory response in fisheries science: when increased fishing mortality reduces intraspecific competition, individuals with the same growth genotypes can grow faster and mature earlier. The difficulty of disentangling such plastic effects and evolutionary changes in empirical data lies at the heart of the debate on fisheries-induced evolution (3, 15–19).

Distinguishing between plastic and genetic responses to harvesting is of considerable practical importance and consequence, because genetic responses (*i*) are often expected to be substantially more difficult and slower to reverse than plastic responses (20–23), (*ii*) alter fundamental processes of population dynamics (24), and (*iii*) could reduce resilience to other stressors such as climate change (25, 26). In addition, there could be economic costs of evolutionary change when fishing mortality is high; alternatively, fisheries-induced evolution can increase profits when fishing mortality is low and a stock's abundance remains above its precautionary level (27). In view of the cumulative and long-term nature of these effects, and in line with a duly precautionary approach to resource management, the potential occurrence of harvest-induced genetic adaptation continues to cause concern (3, 4, 28–30).

Northeast Arctic (NEA) cod (*Gadus morhua*) is one of the world's most important commercial fish stocks and is distributed among feeding grounds in the Barents Sea and spawning grounds

Significance

Rapid anthropogenic trait changes in fish stocks is a highly publicized ocean conservation issue, yet the relative contributions of evolutionary and ecological dynamics are unknown. We present an integrative empirically based simulation model to determine the role of these contributions in the world's largest cod stock. We quantitatively evaluate predictions with different density-dependent growth models using historical stock-specific data. The amount of evolution required for explaining observed maturation trends is small, yet with weakly density-dependent growth, critical for preventing stock collapse. The role of evolution in explaining trends is diminished when density-dependent growth is present. Our study reveals how interactions among evolution, ecology, and fisheries influence stock dynamics and harvest sustainability, emphasizing the need for integrated approaches to fisheries management.

Author contributions: A.M.E., E.S.D., M.H., N.C.S., and U.D. designed research; A.M.E., E.S.D., and M.H. performed research; G.S. contributed analytic tools; A.M.E. and M.H. analyzed data; and A.M.E., E.S.D., M.H., G.S., N.C.S., and U.D. wrote the paper.

Reviewers: A.B., Swedish University of Agricultural Sciences; and T.O.H., Purdue University.

The authors declare no conflict of interest.

Freely available online through the PNAS open access option.

[1]To whom correspondence may be addressed. Email: a.m.eikeset@ibv.uio.no or n.c.stenseth@ibv.uio.no.

This article contains supporting information online at www.pnas.org/lookup/suppl/doi:10.1073/pnas.1525749113/-/DCSupplemental.

along the Norwegian coast. Beginning in the 1930s, a substantial increase in fishing intensity and a change in fishing selectivity occurred as trawlers progressively entered the Barents Sea, exposing smaller immature cod to unprecedented levels of exploitation (31). Until then, coastal fishing with conventional gears had dominated the fishery, mainly targeting mature cod in the spawning grounds (32). In the wake of this striking change in exploitation pattern, the mean age at maturation in NEA cod decreased from more than 9 y in the 1930s to 5–6 y in the 2000s (33–35), a decline far greater than what could be explained by changes in aging methodology or changes in assessing maturation (36). One possible explanation of this precipitous decline is a release from density regulation through reduced biomass levels, resulting in improved conditions for somatic growth and enabling earlier maturation through a compensatory response (e.g., refs. 37 and 38). Another, not mutually exclusive, explanation is that the selective pressures imposed by harvesting have elicited an evolutionary response in the population, causing maturation to be initiated earlier in life and at smaller body sizes (28, 35). Similar considerations apply to other fish stocks, including the collapsed northern cod stock off the east coast of Canada (8). Capitalizing on the striking shift in fishing selectivity experienced by NEA cod, and building on a series of systematic long-term data collected since 1932 (Fig. 1 and Fig. S1*A*), here we evaluate the differential contributions and merits of these two explanatory hypotheses.

In addition to a possible genetic response in maturation schedule, harvesting could induce genetic adaptation in numerous other life history traits (22, 29, 39). For example, evolutionary models have predicted that growth rates could evolve to become either faster or slower, depending on the patterns of size selectivity (22, 40, 41). Harvest could also induce genetic changes in reproductive investment if, for example, intense fishing pressure favors individuals that invest more in current reproduction (5, 22, 42).

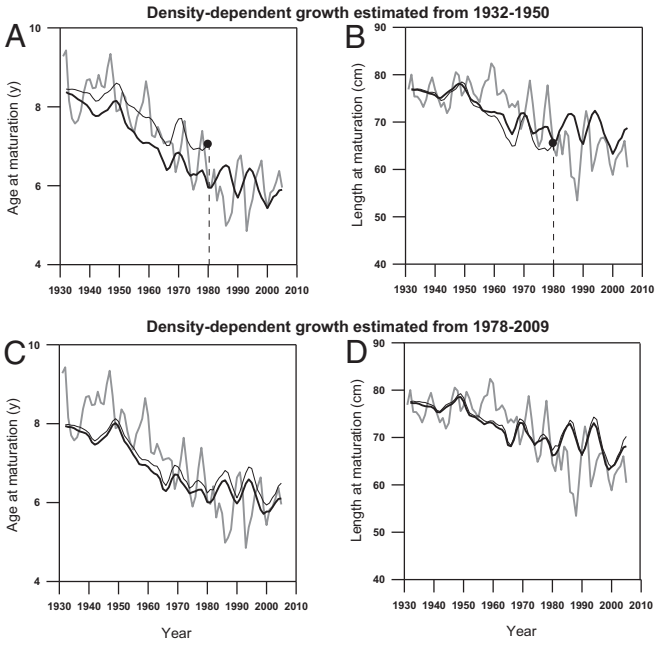

Fig. 1. Comparison of model predictions and observations for age and length at maturation in NEA cod for (*A* and *B*) the historical growth model and (*C* and *D*) the contemporary growth model. Observations are shown with gray lines; eco-evolutionary model predictions, with thick black lines; and nonevolutionary model predictions, with thin black lines. The shown models possess the highest likelihoods among all 16 model variants and associated CV combinations (Table 1 and *S3. Model Selection*). In *A* and *B*, the nonevolving population goes extinct at the point indicated by the filled circles and dashed lines. Model predictions are the mean ages and lengths at maturation among individuals in the population, averaged over 30 independent model runs.

In this study, we use an empirically based multitrait simulation model that integrates ecological and evolutionary dynamics to examine how density-dependent growth and fisheries-induced evolution contribute to the maturation trends observed in NEA cod. Our model enables evolution of key quantitative traits describing the processes of growth, maturation, and reproductive investment. The model has already been used to study optimal harvesting (43) and the bioeconomic consequences of fisheries-induced evolution (27). Including feedbacks between ecological and evolutionary dynamics is a perspective typically missing in fishery science, despite the implications for management (44). We address this challenge using extensive time series data collected for an important marine fish stock (4). Our main objective and key contribution are to assess the levels of density-dependent growth and fisheries-induced evolution required for achieving good agreement between model predictions and a 74-y time series of age and length at maturation. We extend earlier work in three key directions. First, although eco-evolutionary models have included density-dependent growth (24, 45–48), previous evolutionary models of NEA cod (28, 49–51) did not, and thus could not assess the differential contributions of phenotypic plasticity and trait evolution to the observed maturation trends in this stock. Second, although some eco-evolutionary models have allowed simultaneous evolution of multiple traits (e.g., growth and maturation) (22, 45, 46, 48, 52), most previous studies restricted attention to the evolution of maturation schedules (51, 53–56); here, we consider an evolving maturation schedule in conjunction with the potential for fisheries-induced evolution in two other important life history traits, somatic growth and reproductive investment. Allowing for the simultaneous evolution of these additional traits might reduce the amount of evolution predicted in the maturation schedule, because the processes of growth, maturation, and reproductive investment are naturally intertwined. Third, to our knowledge, previous studies have not statistically compared stock-specific time series data with model predictions, as we do here to evaluate the relative roles of fisheries-induced evolution and density-dependent growth.

To consider the importance of density dependence for the dynamics of NEA cod, we investigate two density-dependent growth models. The first model (the "contemporary growth model") is estimated for the later part of the time series for which the data allow for a direct estimation of the density dependence of growth (1978–2009), revealing a strong, negative relationship with a high degree of variation explained (*S1. Model Description*). Because this relationship might not be representative of historical conditions, we also estimate a second model (the "historical growth model") for the beginning of the time series (1932–1950) when the population was larger: the earlier data do not allow for the direct estimation of growth and probably underestimate the strength of its density dependence, but nevertheless suggests a much weaker density dependence of growth, albeit with poorer explanatory power (*S1. Model Description*). The choice of these two time periods provides a good contrast between the two corresponding growth models (i.e., strong versus weak density dependence), enabling us to evaluate the potential role of density-dependent growth using parameters empirically derived for a large marine fish stock.

Our simulation model includes four evolving life history traits: somatic growth capacity, reproductive investment (measured by the gonadosomatic index, GSI), and the intercept and slope of the probabilistic maturation reaction norm (PMRN) characterizing the maturation schedule (10, 12, 34). For both growth models and all evolving traits, we analyze the effects of different coefficients of genetic variation (CV), ranging from 0% to 14% in the initial population. The CV is a measure of the scope for evolution in a given trait (24, 27). When the CVs for all genetic

traits are set to 0, the model is nonevolutionary and stock dynamics are driven solely by ecological processes including density-dependent growth. Larger CVs enable a stronger contribution from fisheries-induced evolution (22). Using the fishing mortalities estimated for NEA cod for 1932–2006 (*S1. Model Description* and Fig. S1*A*), we analyze how the model's capacity to match the observed maturation trends varies with these CVs (Table 1 and Table S1).

Although eco-evolutionary models have been used to investigate fisheries-induced evolution, the present study is unique because of its tight coupling of long-term time series data for a wild fish stock with the retrospective simulation of the stock's dynamics based on a carefully calibrated model; this is a different approach from other, more strategic or general, models of life history evolution (22, 23, 51, 57). Crucially, we let the data "decide" on the most plausible levels of evolution, by determining which values of CV maximize the fit (measured through the likelihood function) between the model and the data.

Results

When using the historical growth model (describing weak density dependence), the nonevolutionary model with all four CVs set to 0 predicts stock collapse (i.e., population extinction) around 1980, which obviously did not happen in reality (Fig. 1 *A* and *B*). Even when considering an alternative maturation schedule (obtained by pooling the PMRNs of cohorts from 1932 to 2005, which results in higher survival, earlier maturation, and the avoidance of stock collapse in the nonevolutionary model), the match with the empirical maturation trends remains very poor when evolution is absent and the historical growth model is used (*S4. Alternative Maturation Model*, Fig. S2, and Table S2). In contrast, the best (likelihood maximizing) evolutionary model variant when using the historical growth model reproduces the observed trends in age and length at maturation well (Fig. 1 *A* and *B*). These findings support the hypothesis that trait evolution has contributed to the stock's dynamics during the 20th century, assuming that the historic density-dependent growth relationship is accurate.

When using the contemporary growth model (describing strong density dependence), a model variant with low CVs performs best (by likelihood), suggesting that, for this growth model, a good match with the data can be achieved with little fisheries-induced evolution (Fig. 1 *C* and *D*). This is possible because with stronger density dependence, fishing results in significantly faster growth, which in turn promotes significantly earlier maturation via phenotypic plasticity. This greater scope for growth-related maturation plasticity means that less evolution is required to explain the observed maturation trends.

The top-ranked model variants are similar when evaluated using the Akaike information criterion (AIC), which combines a measure of fit to the data (likelihood) with a penalty (58) for each positive CV (Table 1). In these model variants, the CVs for the two maturation traits are consistently low (0% or 2%), and this also applies to the CVs for reproductive investment (0–4%), regardless of the applied growth model (Table 1). In the top-ranked model variants, the CVs for growth are consistently high (14%) when the historical growth model is used, but consistently low (0–4%) when the contemporary growth model is used (Table 1). This occurs because more growth evolution is required to match the observed maturation trends when the density dependence of growth is weak. For the top-ranked evolutionary model variants, we can thus conclude as follows. First, the PMRN intercept shows a slow and steady evolutionary decline from 1950 onward, because selection from the feeding-ground fishery favors earlier maturation (Fig. S3*A*). Second, the PMRN slope and GSI evolve very little, with the GSI showing a tendency to increase over time (Table 1 and Fig. S3 *B* and *C*). Third, growth capacity evolves more quickly, particularly when the historical growth model is used (Fig. S3*D*).

Although the model variants are selected solely based on matching the empirical time series of age and length at maturation, they perform well in predicting the empirical time series of other stock characteristics, including length at age (Fig. S4), phenotypic growth rate (Fig. S5*A*), and recruitment at age 3 y (Fig. S5*B*). However, although the overall qualitative trends are similar, the total stock biomass estimated from a stock assessment model consistently exceeds that predicted by our model (Fig. S5*C* and *S6. Comparison with Other Observed Trends*).

Also, our model generally matches the spawning stock biomass estimated from the stock assessment model during the earlier part of the time series, but less well in recent years (Fig. S5*D*).

Table 1. Top-ranked model variants with their CVs for the four considered life history traits (i, PMRN intercept; g, growth capacity; GSI, gonadosomatic index; s, PMRN slope)

CV					
CV_i	CV_s	CV_g	CV_{GSI}	Log-likelihood, ln *L*	AIC difference
i) Historical density-dependent growth model					
0.02	**0.06**	**0.14**	**0.02**	**−177.74***	1.7
0.02	*0*	*0.14*	*0.08*	−177.88	*0*
ii) Contemporary density-dependent growth model					
0.02	**0.1**	**0.04**	**0.12**	**−181.22***	2.9
0.02	*0*	*0*	*0*	−182.75	*0*

Two alternative density-dependent growth models are considered: (*i*) the historical growth model and (*ii*) the contemporary growth model. The models are ranked by their log-likelihood ln *L* (higher is better) and AIC relative to the model variant with the lowest AIC (lower is better). For each growth model, the best-fitting model variants are shown (in bold for the maximum likelihood and in italics for the lowest AIC). For an extended version of this table, see Table S1.

*Having maximum likelihoods, these model variants are shown in Fig. 1.

Discussion

The world's largest cod stock, NEA cod, was recently reported to be at the highest biomass levels ever recorded (59). Other fish stocks, like those of northern cod around Newfoundland, have collapsed due to, among other factors, high fishing pressure (60, 61). However, although NEA cod has historically also experienced high fishing pressures, with a mean fishing probability of 49% per year from 1932 to 2006 (27), it has persisted and even thrived. There are likely multiple reasons for the continued success of the NEA cod fishery, but the predictions of our model suggest, in the case of weakly density-dependent growth, that evolution has contributed to preventing stock collapse and sustaining the substantial fishing pressure the stock has experienced. However, our analyses show that density-dependent growth is also critically important for interpreting the observed trends in life history traits and stock dynamics. This is highlighted by how predictions differ depending on whether the density dependence of growth is assumed to be strong or weak. When growth is strongly density dependent (i.e., for the contemporary growth model), the performance of the nonevolutionary model and best-fitting evolutionary model variants are statistically similar. Even though some of the tested evolutionary model variants fit the data better (i.e., had a higher likelihood and a lower AIC) than the corresponding nonevolutionary model, the AIC difference of 0.6 between the nonevolutionary model and the evolutionary model variant with lowest AIC is small (and in this case, only one CV was positive, yet small) (Table 1). It is generally accepted that all models within an AIC difference of 2 of the best-fitting model have similar empirical support (e.g., ref. 58).

Several other predictions are sensitive to the growth model used (Table 1 and Fig. S1*B*). Most importantly, stock collapse

(i.e., population extinction) is predicted when the density dependence in growth is assumed to be as weak as that estimated for the historical period and there is no concurrent evolution. Furthermore, the historical growth model predicts much more growth evolution than the contemporary growth model (Fig. S3*D*). The reason is that the historical trends in age and length at maturation can partly be explained by increased phenotypic growth, which can arise in two ways: growth is strongly density dependent (so the reduction in biomass from fishing enables faster phenotypic growth) or growth evolves to be faster. Therefore, the best-fitting model variants have a high CV of growth if growth is weakly density dependent or a low CV of growth if growth is strongly density dependent.

Although it is not possible to determine with certainty which growth model is more accurate, the weight of evidence suggests that the contemporary growth model is more reliable. The contemporary growth model has a high explanatory power and enables a superior fit to the observed trends in length at age (especially for older ages; Fig. S4), supporting a model with strongly density-dependent growth and less growth evolution. Importantly, the quality of the data used to estimate the contemporary growth model is higher and additional environmental variables could be accounted for (*S1. Model Description*), lending good empirical support to this model and providing evidence for more strongly density-dependent growth. However, aquaculture studies of Atlantic cod (62, 63) suggest a high genetic variance in growth, and previous studies of other species found evidence for harvest-induced evolution of growth (10, 29, 64, 65), suggesting that weaker density dependence and more evolution of growth are possible. Another possibility is that the strength of density-dependent growth has varied over time, which could happen if, for example, ecosystem conditions have changed (66, 67).

Our analyses reveal less fisheries-induced evolution in NEA cod than previous studies of this and other marine fish stocks (3, 8, 35, 68). In particular, our model variants with higher CVs of the maturation traits produce poorer matches with the time series data. This could indicate a large contribution from phenotypic plasticity in explaining historical dynamics in NEA cod, with less contribution from evolutionary change than previously thought (28, 35, 50, 51). As a result of lower CVs, PMRN evolution predicted by our top-ranking model variants is considerably slower and smaller in magnitude than predicted by other eco-evolutionary models (22–24, 55). However, those previous models were not specific to NEA cod; for example, two of these models were for a generic Atlantic cod stock (22, 23) and one was for smallmouth bass (55). When examining CVs similar to those assumed in these previous models, we also predict more PMRN evolution; but by comparing with empirical data, these higher rates of evolution result in unrealistically low ages and lengths at maturation for this stock (27) (Fig. S6). The overall magnitude of change in the PMRN found in our study is also smaller than what has been previously inferred for NEA cod (35), as well as for other fish stocks (8, 65, 68–70). It is only by statistically matching our model predictions with empirical trends under different scenarios of density dependence that we come to these different conclusions about the likely magnitude of fisheries-induced evolution in NEA cod.

The reasons why previous empirical estimates of PMRN dynamics differ from our model-predicted PMRN trends are unclear. However, we can point out several key assumptions that may contribute. First, the PMRNs of individuals are genetic traits in our model, whereas empirical estimates of PMRNs are based on phenotypic data, which themselves are subject to measurement error (including unaccounted environmental effects) and other assumptions (11). Second, we assume linear PMRNs, whereas empirically estimated PMRNs can be nonlinear. Because PMRNs can often be estimated only for a few ages, robust extrapolation of their shapes beyond the empirically well-covered age range is not possible, hampering the identification of nonlinearities in their shapes. Nevertheless, the nonlinearities of empirically estimated cod PMRNs are not strong (9, 34, 35) and are therefore unlikely to have a large impact on maturation dynamics. Third, increasing the CVs of the PMRN intercept and slope—in our current model implementation—widens the population-level PMRN, and thereby enables earlier maturation. An alternative way of implementing increases in these two CVs is to simultaneously reduce the individual-level variability in maturation, such that the population-level variability remains unchanged (*S7. Higher Genetic Variances*). This could favor higher CVs of the PMRN intercept and slope among the best-fitting model variants and result in better agreement with the estimated PMRN trends, offering an interesting challenge for future research (*S8. Model Limitations*).

Our model predicts the evolution of increased growth capacity, a finding that might seem unexpected given earlier experiments (29, 71, 72) but is in agreement with model-based studies (22, 23, 40, 73) and theory (39). A closer look reveals a logical explanation for faster growth. In most fish, growing faster causes maturation earlier in life. By evolving a higher growth capacity, individuals can thus mature earlier, with a higher probability of reproducing before being caught by the fishery. Such a response is expected to occur when the fishery's minimum-size limit is low enough that both immature and mature fish are harvested (22, 40), as is the case for NEA cod in the feeding grounds. By allowing growth capacity to evolve and by including phenotypic plasticity in maturation, we capture this selection pressure. Our model predictions are strengthened by their good match with data on length at age (Fig. S4) and on phenotypic growth (Fig. S5*A*). For NEA cod, phenotypic trends toward faster somatic growth (implying larger lengths at age) have indeed been documented for older age groups (74, 75). The recognition that model-predicted maturation evolution is altered by growth evolution strengthens the case for including multiple evolving traits in life history models.

Although our model predicts a genetically based increase in reproductive investment (GSI), the magnitude of this evolutionary change is so small that it would be difficult to detect in the wild. This finding is in accordance with empirical data: liver weight (standardized for body length) in NEA cod, a possible proxy of the energy available for reproduction (76), exhibited no more than a weak overall increase from 1946 to 2001 (75). Furthermore, no consistent temporal trends in reproductive investment have been detected (77), and as far as we know, no other empirical data published to date suggest genetically based changes in reproductive investment in NEA cod. Previous eco-evolutionary models have also predicted less fisheries-induced evolution of reproductive investment than for PMRNs or growth (22).

Although our eco-evolutionary model is not the only one to address density-dependent growth simultaneously with life history evolution (24, 47, 57, 78), it quantitatively links model results to life history changes that have unfolded in a wild fish population as it was harvested. By mimicking the observed annual fishing mortalities experienced by this stock (Fig. S1*A*), we are capturing underlying interactions between the resource and human behavior, as the historical fishing pattern is the outcome of how humans (e.g., fishers, managers, and society), among other factors, have interacted with the stock as it changed over time. This is an added dimension that, although important, is typically neglected in most biological models used to predict trends in exploited populations and is another reason why tight coupling with empirical data is so powerful.

The model we present succeeds in capturing important aspects of the NEA cod stock's response to harvest, highlighting the necessity of including key feedbacks between ecology and evolution. For example, the evolution of growth, often left out of models of fisheries-induced evolution, plays a prominent role in matching stock dynamics because of its interaction with maturation and

reproduction. We conclude that it is the simultaneous consideration of ecological and evolutionary dynamics that is required to explain the full breadth of observed trends. By using an empirically grounded eco-evolutionary life history model of NEA cod, we have shown that, although some evolution is needed to prevent stock collapse and therefore sustain harvest, density-dependent growth could account for much of the maturation change observed in this stock. Our approach serves as an example of how the tight coupling of a calibrated eco-evolutionary model with empirical time series data can be used as a tool for designing sustainable harvest regimes as part of an integrated approach to ecosystem-based management.

Materials and Methods

Our eco-evolutionary model describes the life cycle of NEA cod. It is built upon the model framework described by ref. 22, and a full description of the model can be found in ref. 27. We therefore only focus on key elements below and provide additional details in the *S1. Model Description*. The model is eco-genetic, containing ecological and genetic details that describe key features of an individual's life cycle, including birth and inheritance, growth of soma and gonads, sexual maturation, reproduction, and natural and fishing mortality. It is empirically based and has multiple evolving life history traits that are expressed phenotypically, allowing for environmental variation and phenotypic plasticity to influence observed trait values. We model differential mortality regimes experienced by the stock in spawning and feeding grounds, but include no other spatial structure. The model is defined by statistical relationships and parameter values derived from empirical data available for NEA cod, including time series of fishing mortalities, density-dependent growth, and recruitment from 1932 to 2006.

Our model describes quantitative inheritance and evolution of four life history traits: somatic growth capacity, reproductive investment (measured by the GSI), and the intercept and slope of the PMRN. Offspring inherit genetic trait values from their parents assuming normally distributed genetic variation around the midparental values (with the corresponding variance for each genetic trait equaling one-half of its genetic variance in the initial population), describing the effects of recombination, segregation, and mutation (22, 27). The genetic trait values are expressed by drawing normally distributed phenotypic trait values with variances that equal the interindividual environmental variance estimated for each trait. Interannual environmental variation is included in the model through density-dependent growth. Genotypes that better enable survival and reproduction will be selected for over time, changing the stock's trait distributions. Emergent trait phenotypes of special interest are the age and length at maturation. If the genetic trait values affecting these phenotypic traits change over time, trends in the stock's mean age and length at maturation have an evolutionary component.

Phenotypic plasticity occurs when a genotype is expressed as different phenotypes as a function of the environment (79). We include phenotypic plasticity in our model through density-dependent growth and PMRNs. Density-dependent growth is included to account for the expected increase in per capita resource availability as population biomass is reduced by fishing (59). Density-dependent growth has been observed in many species, including marine fish stocks (80), and our parameter estimation using time series data provides empirical support that it also occurs in NEA cod (*S1. Model Description*). In our model, an individual's phenotypically expressed growth rate is determined by reducing its genetic growth capacity as a function of population biomass. As phenotypic growth rates change with population biomass, the age and length at maturation shift along the PMRN (11).

The derivation of parameter values is fully described in ref. 27, with the most pertinent details highlighted here (all model parameters are listed in the *S2. Model Parameterization*). The initial population-level mean trait values for the genetic traits are estimated from empirical data; the resultant genetic trait distributions of individuals in the population are then free to change through time depending on selection. A unique feature of this study is the comparison between two different density-dependent growth models, the parameters of which are determined empirically (*S1. Model Description*). For the historical growth model, we assume a relationship estimated from data for 1932–1950. As fishing mortalities were lower during this time and because of the averaging that is inherent in estimating this model, the density dependence of growth inferred for this period is weaker. For the contemporary growth model, we assume a relationship estimated from data for 1978–2009. The density dependence of growth inferred for this contemporary period is stronger. To mimic the fishing pressure experienced by the stock, we use data on the annual fishing mortalities in the feeding grounds and spawning grounds from 1932 to 2005 (*S1. Model Description*).

The CV of a trait directly influences the rate of evolution and is equal to the genetic SD of the trait divided by the trait's mean value (22, 55, 81, 82). To evaluate models with alternative rates of evolution, we vary the CV of each of the four traits in the initial population (24) independently from 0% to 14% in steps of 2% (ideally, optimization should be performed over the whole continuous range of CV values; restriction to a discrete set of values was chosen due to computational costs). Thus, $2^4 = 16$ model variants are analyzed (resulting from choosing a zero or positive CV value for each of the four traits) based on $8^4 = 4{,}096$ CV combinations (resulting from considering eight CV values for each of the four traits). Consequently, one model variant and one CV combination describe stock dynamics without any evolution (i.e., with all four CVs equaling zero), whereas all others correspond to evolution being possible in at least one of the traits. Each CV combination is run for 30 independent replicates (resulting in a total of $4{,}096 \times 30 = 122{,}880$ model runs) and their results are averaged for that CV combination. The performances of all model variants and associated CV combinations are statistically evaluated, using the likelihood function and the AIC, by comparing model predictions for annual mean ages and lengths at maturation with 74 y of observations on maturation in NEA cod (*S3. Model Selection*).

ACKNOWLEDGMENTS. We are grateful to the Research Computing Services at the University of Oslo for access to computing resources crucial for this study. We thank A. Hylen, K. Nedreaas, B. Bogstad, and O. S. Kjesbu for kindly providing data on biomass and reproduction, and C. T. Marshall for data on length at age. We sincerely appreciate comments provided by J. Hutchings, C. T. Marshall, N. L. Hjort, O. R. Godø, T. Hansen, B. Shuter, K. Brander, and E. Kenchington, and discussions with K. Enberg and C. Jørgensen on the model and results. This work was supported by the Norwegian Research Council (A.M.E., E.S.D., M.H., and N.C.S.), NordForsk (GreenMAR) (A.M.E. and N.C.S.), the Bergen Research Foundation (M.H.), the European Research Training Network on Fisheries-Induced Adaptive Changes in Exploited Stocks (FishACE; Grant MRTN-CT-2204-005578) (to E.S.D., M.H., and U.D.), the European Specific Targeted Research Programme on Fisheries-induced Evolution (FinE; Grant SSP-2006-044276) (to A.M.E., E.S.D., M.H., N.C.S., and U.D.), the European Science Foundation (U.D.), the Austrian Science Fund (U.D.), the Austrian Ministry of Science and Research (U.D.), and the Vienna Science and Technology Fund (U.D.).

1. Coltman DW, et al. (2003) Undesirable evolutionary consequences of trophy hunting. *Nature* 426(6967):655–658.
2. Tenhumberg B, Tyre AJ, Pople AR, Possingham HP (2004) Do harvest refuges buffer kangaroos against evolutionary responses to selective harvesting? *Ecology* 85(7):2003–2017.
3. Jørgensen C, et al. (2007) Ecology: Managing evolving fish stocks. *Science* 318(5854): 1247–1248.
4. Schoener TW (2011) The newest synthesis: Understanding the interplay of evolutionary and ecological dynamics. *Science* 331(6016):426–429.
5. Roff DA (1992) *The Evolution of Life Histories: Theory and Analysis* (Chapman and Hall, New York).
6. Haugen TO, Vøllestad LA (2001) A century of life-history evolution in grayling. *Genetica* 112-113:475–491.
7. Grift RE, Rijnsdorp AD, Barot S, Heino M, Dieckmann U (2003) Fisheries-induced trends in reaction norms for maturation in North Sea plaice. *Mar Ecol Prog Ser* 257:247–257.
8. Olsen EM, et al. (2004) Maturation trends indicative of rapid evolution preceded the collapse of northern cod. *Nature* 428(6986):932–935.
9. Heino M, Dieckmann U, Godø OR (2002) Measuring probabilistic reaction norms for age and size at maturation. *Evolution* 56(4):669–678.
10. Swain DP, Sinclair AF, Mark Hanson J (2007) Evolutionary response to size-selective mortality in an exploited fish population. *Proc Biol Sci* 274(1613):1015–1022.
11. Dieckmann U, Heino M (2007) Probabilistic maturation reaction norms: Their history, strengths, and limitations. *Mar Ecol Prog Ser* 335:253–269.
12. Browman HI, Law R, Marshall CT (2008) The role of fisheries-induced evolution. *Science* 320(5872):47–50, author reply 47–50.
13. Pelletier F, Garant D, Hendry AP (2009) Eco-evolutionary dynamics. *Philos Trans R Soc Lond B Biol Sci* 364(1523):1483–1489.
14. Post DM, Palkovacs EP (2009) Eco-evolutionary feedbacks in community and ecosystem ecology: Interactions between the ecological theatre and the evolutionary play. *Philos Trans R Soc Lond B Biol Sci* 364(1523):1629–1640.
15. Hilborn R (2006) Faith-based fisheries. *Fisheries (Bethesda, Md)* 31(11):554–555.
16. Conover DO, Munch SB (2007) Faith, evolution, and the burden of proof. *Fisheries (Bethesda, Md)* 32(2):90–91.
17. Darimont CT, et al. (2009) Human predators outpace other agents of trait change in the wild. *Proc Natl Acad Sci USA* 106(3):952–954.
18. Kinnison MT, et al. (2009) Some cautionary notes on fisheries evolutionary impact assessments. *Proc Natl Acad Sci USA* 106(41):E115–author reply E116.
19. Cameron TC, O'Sullivan D, Reynolds A, Piertney SB, Benton TG (2013) Eco-evolutionary dynamics in response to selection on life-history. *Ecol Lett* 16(6):754–763.
20. de Roos AM, Boukal DS, Persson L (2006) Evolutionary regime shifts in age and size at maturation of exploited fish stocks. *Proc Biol Sci* 273(1596):1873–1880.

21. Conover DO, Munch SB, Arnott SA (2009) Reversal of evolutionary downsizing caused by selective harvest of large fish. *Proc Biol Sci* 276(1664):2015–2020.
22. Dunlop ES, Heino M, Dieckmann U (2009) Eco-genetic modeling of contemporary life-history evolution. *Ecol Appl* 19(7):1815–1834.
23. Enberg K, Jørgensen C, Dunlop ES, Heino M, Dieckmann U (2009) Implications of fisheries-induced evolution for stock rebuilding and recovery. *Evol Appl* 2(3):394–414.
24. Dunlop ES, Eikeset AM, Stenseth NC (2015) From genes to populations: How fisheries-induced evolution alters stock productivity. *Ecol Appl* 25(7):1860–1868.
25. Jørgensen C, Dunlop ES, Opdal AF, Fiksen O (2008) The evolution of spawning migrations: State dependence and fishing-induced changes. *Ecology* 89(12):3436–3448.
26. Hsieh CH, Yamauchi A, Nakazawa T, Wang WF (2010) Fishing effects on age and spatial structures undermine population stability of fishes. *Aquat Sci* 72(2):165–178.
27. Eikeset AM, Richter A, Dunlop ES, Dieckmann U, Stenseth NC (2013) Economic repercussions of fisheries-induced evolution. *Proc Natl Acad Sci USA* 110(30):12259–12264.
28. Law R, Grey DR (1989) Evolution of yields from populations with age-specific cropping. *Evol Ecol* 3:343–359.
29. Conover DO, Munch SB (2002) Sustaining fisheries yields over evolutionary time scales. *Science* 297(5578):94–96.
30. Palkovacs EP, Kinnison MT, Correa C, Dalton CM, Hendry AP (2012) Fates beyond traits: Ecological consequences of human-induced trait change. *Evol Appl* 5(2):183–191.
31. Godø OR (2003) Fluctuation in stock properties of north-east Arctic cod related to long-term environmental changes. *Fish Fish* 4:121–137.
32. Sætersdal G, Hylen A (1964) The decline of the skrei fisheries. *FiskDir Skr Ser Havunder* 13(7):56–69.
33. Godø OR (2000) *Maturation Dynamics of Arcto-Norwegian Cod* (International Institute for Applied Systems Analysis, Laxenburg, Austria), IIASA Interim Report IR-00-024.
34. Heino M, Dieckmann U, Godø OR (2002) Estimating reaction norms for age and size at maturation with reconstructed immature size distributions: A new technique illustrated by application to northeast Arctic cod. *ICES J Mar Sci* 59(3):562–575.
35. Heino M, Dieckmann U, Godø OR (2002) Reaction norm analysis of fisheries-induced adaptive change and the case of the Northeast Arctic cod (International Council for the Exploration of the Sea, Copenhagen), ICES CM 2002/Y:14.
36. Zuykova AV, et al. (2009) Age determination of northeast Arctic cod otoliths through 50 years of history. *Mar Biol Res* 5(1):66–74.
37. Godø OR, Moksness E (1987) Growth and maturation of Norwegian coastal cod and northeast Arctic cod under different conditions. *Fish Res* 5:235–242.
38. Jørgensen T (1990) Long-term changes in age at sexual maturity of northeast Arctic cod (*Gadus morhua* L). *ICES J Mar Sci* 46(3):235–248.
39. Enberg K, et al. (2012) Fishing-induced evolution of growth: Concepts, mechanisms and the empirical evidence. *Mar Ecol (Berl)* 33(1):1–25.
40. Andersen KH, Brander K (2009) Expected rate of fisheries-induced evolution is slow. *Proc Natl Acad Sci USA* 106(28):11657–11660.
41. Traill LW, Schindler S, Coulson T (2014) Demography, not inheritance, drives phenotypic change in hunted bighorn sheep. *Proc Natl Acad Sci USA* 111(36):13223–13228.
42. Reznick DA, Bryga H, Endler JA (1990) Experimentally induced life-history evolution in a natural population. *Nature* 346:357–359.
43. Eikeset AM, et al. (2013) A bio-economic analysis of harvest control rules for the northeast Arctic cod fishery. *Mar Policy* 39:172–181.
44. Fraser DJ (2013) The emerging synthesis of evolution with ecology in fisheries science. *Can J Fish Aquat Sci* 70(9):1417–1428.
45. Wang HY, Höök TO (2009) Eco-genetic model to explore fishing-induced ecological and evolutionary effects on growth and maturation schedules. *Evol Appl* 2(3):438–455.
46. Piou C, Prevost E (2012) A demo-genetic individual-based model for Atlantic salmon populations: Model structure, parameterization and sensitivity. *Ecol Modell* 231:37–52.
47. Vainikka A, Hyvärinen P (2012) Ecologically and evolutionarily sustainable fishing of the pikeperch *Sander lucioperca*: Lake Oulujärvi as an example. *Fish Res* 113(1):8–20.
48. Castellani M, et al. (2015) IBSEM: An individual-based Atlantic salmon population model. *PLoS One* 10(9):e0138444.
49. Heino M (1998) Management of evolving fish stocks. *Can J Fish Aquat Sci* 55:1971–1982.
50. Jørgensen C, Ernande B, Fiksen Ø (2009) Size-selective fishing gear and life history evolution in the northeast Arctic cod. *Evol Appl* 2(3):356–370.
51. Zimmermann F, Jørgensen C (2015) Bioeconomic consequences of fishing-induced evolution: A model predicts limited impact on net present value. *Can J Fish Aquat Sci* 72(4):612–624.
52. Bromaghin JF, Nielson RM, Hard JJ (2011) A model of chinook salmon population dynamics incorporating size-selective exploitation and inheritance of polygenic correlated traits. *Nat Res Mod* 24:1–47.
53. Baskett ML, Levin SA, Gaines SD, Dushoff J (2005) Marine reserve design and the evolution of size at maturation in harvested fish. *Ecol Appl* 15(3):882–901.
54. Gårdmark A, Dieckmann U (2006) Disparate maturation adaptations to size-dependent mortality. *Proc Biol Sci* 273(1598):2185–2192.
55. Dunlop ES, Shuter BJ, Dieckmann U (2007) Demographic and evolutionary consequences of selective mortality: Predictions from an eco-genetic model for smallmouth bass. *Trans Am Fish Soc* 136:749–765.
56. Kuparinen A, Stenseth NC, Hutchings JA (2014) Fundamental population-productivity relationships can be modified through density-dependent feedbacks of life-history evolution. *Evol Appl* 7(10):1218–1225.
57. Ivan LN, Höök TO (2015) Energy allocation strategies of young temperate fish: An eco-genetic modeling approach. *Can J Fish Aquat Sci* 72(8):1243–1258.
58. Burnham KP, Anderson DR (2002) *Model Selection and Multimodel Inference: A Practical Information-Theoretic Approach* (Springer, New York).
59. Kjesbu OS, et al. (2014) Synergies between climate and management for Atlantic cod fisheries at high latitudes. *Proc Natl Acad Sci USA* 111(9):3478–3483.
60. Hutchings JA, Myers R (1994) What can be learned from the collapse of a renewable resource? Atlantic cod, *Gadus morhua*, of Newfoundland and Labrador. *Can J Fish Aquat Sci* 51(9):2126–2146.
61. Hutchings JA (2000) Collapse and recovery of marine fishes. *Nature* 406(6798):882–885.
62. Gjerde B, Terjesen BT, Barr Y, Lein I, Thorland I (2004) Genetic variation for juvenile growth and survival in Atlantic cod (*Gadus morhua*). *Aquaculture* 236:1667–1177.
63. Bangera R, et al. (2015) Genotype by environment interaction for growth in Atlantic cod (*Gadus morhua* L.) in four farms of Norway. *J Mar Sci Eng* 3(2):412–427.
64. Nusslé S, Bornand CN, Wedekind C (2009) Fishery-induced selection on an Alpine whitefish: Quantifying genetic and environmental effects on individual growth rate. *Evol Appl* 2(2):200–208.
65. Pardoe H, Vainikka A, Thordarson G, Marteinsdottir G, Heino M (2009) Temporal trends in probabilistic maturation reaction norms and growth of Atlantic cod (*Gadus morhua*) on the Icelandic shelf. *Can J Fish Aquat Sci* 66:1719–1733.
66. Gobin J, Lester NP, Cottril A, Fox MG, Dunlop ES (2015) Trends in growth and recruitment of Lake Huron lake whitefish during a period of ecosystem change, 1985 to 2012. *J Great Lakes Res* 41(2):405–414.
67. Casini M, Rouyer T, Bartolino V, Larson N, Grygiel W (2014) Density-dependence in space and time: Opposite synchronous variations in population distribution and body condition in the Baltic Sea sprat (*Sprattus sprattus*) over three decades. *PLoS One* 9(4):e92278.
68. Sharpe DM, Hendry AP (2009) Life history change in commercially exploited fish stocks: An analysis of trends across studies. *Evol Appl* 2(3):260–275.
69. Vainikka A, Gårdmark A, Bland B, Hjelm J (2009) Two- and three-dimensional maturation reaction norms for the eastern Baltic cod, *Gadus morhua*. *ICES J Mar Sci* 66:248–257.
70. Feiner ZS, et al. (2015) Rapidly shifting maturation schedules following reduced commercial harvest in a freshwater fish. *Evol Appl* 8(7):724–737.
71. Reznick DN, Ghalambor CK (2005) Can commercial fishing cause evolution? Answers from guppies. *Can J Fish Aquat Sci* 62:791–801.
72. van Wijk SJ, et al. (2013) Experimental harvesting of fish populations drives genetically based shifts in body size and maturation. *Front Ecol Environ* 11(4):181–187.
73. Dunlop ES, Baskett ML, Heino M, Dieckmann U (2009) Propensity of marine reserves to reduce the evolutionary effects of fishing in a migratory species. *Evol Appl* 2(3):371–393.
74. Jørgensen T (1992) Long-term changes in growth of North-east Arctic cod (*Gadus morhua*) and some environmental influences. *ICES J Mar Sci* 49:263–277.
75. Marshall CT, Needle CL, Yaragina NA, Ajiad AM, Gusev E (2004) Deriving condition indices from standard fisheries databases and evaluating their sensitivity to variation in stored energy reserves. *Can J Fish Aquat Sci* 61(10):1900–1917.
76. Yoneda M, Wright PJ (2004) Temporal and spatial variation in reproductive investment of Atlantic cod *Gadus morhua* in the northern North Sea and Scottish west coast. *Mar Ecol Prog Ser* 276:237–248.
77. Kjesbu OS, Witthames PR, Solemdal P, Walker MG (1998) Temporal variations in the fecundity of Arcto-Norwegian cod (*Gadus morhua*) in response to natural changes in food and temperature. *J Sea Res* 40(3-4):303–321.
78. Marty L, Dieckmann U, Ernande B (2015) Fisheries-induced neutral and adaptive evolution in exploited fish populations and consequences for their adaptive potential. *Evol Appl* 8(1):47–63.
79. Pigliucci M (2005) Evolution of phenotypic plasticity: Where are we going now? *Trends Ecol Evol* 20(9):481–486.
80. Lorenzen K, Enberg K (2002) Density-dependent growth as a key mechanism in the regulation of fish populations: Evidence from among-population comparisons. *Proc Biol Sci* 269(1486):49–54.
81. Houle D (1992) Comparing evolvability and variability of quantitative traits. *Genetics* 130(1):195–204.
82. Mousseau TA, Roff DA (1987) Natural selection and the heritability of fitness components. *Heredity (Edinb)* 59(Pt 2):181–197.
83. McEvoy LA, McEvoy J (1992) Multiple spawning in several commercial fish species and its consequences for fisheries management, cultivation and experimentation. *J Fish Biol* 41:125–136.
84. ICES (2009) *Report of the Arctic Fisheries Working Group (AFWG), 21–27 April 2009, San-Sebastian, Spain* (International Council for the Exploration of the Sea, Copenhagen), ICES CM 2009/ACOM:01.
85. Hylen A (2002) Fluctuations in abundance of northeast Arctic cod during the 20th century. *ICES Mar Sci Symp* 215:543–550.
86. Akaike H (1974) A new look at statistical model identification. *IEEE Trans Automat Contr* AU-19:716–722.
87. Aglen A, Drevetnyak K, Sokolov K (2004) Cod in the Barents Sea (northeast Arctic cod)—a review of the biology and history of the fishery and its management. *Proceedings of the 10th Norwegian–Russian Symposium*, eds Bjordal Å, Gjøsæter H, Mehl S (Institute of Marine Research, Bergen, Norway; Polar Research Institute of Marine Fisheries and Oceanography, Murmansk, Russia), pp 27–39.
88. Huse G, Johansen GO, Bogstad B, Gjøsæter H (2004) Studying spatial and trophic interactions between capelin and cod using individual-based modelling. *ICES J Mar Sci* 61:1201–1213.
89. Scheffer M, Baveco JM, Deangelis DL, Rose KA, Vannes EH (1995) Super-individuals as a simple solution for modeling large populations on an individual basis. *Ecol Modell* 80(2-3):161–170.
90. Devore JL, Berk KN (2012) *Modern Mathematical Statistics with Applications* (Springer, New York), 2nd Ed.
91. ICES (2013) *Report of the Arctic Fisheries Working Group 2013 (AFWG), 18–24 April 2012, ICES Headquarters, Copenhagen* (International Council for the Exploration of the Sea, Copenhagen), ICES CM 2013/ACOM:05.
92. Hjermann DO, et al. (2007) Food web dynamics affect northeast Arctic cod recruitment. *Proc Biol Sci* 274(1610):661–669.
93. Korsbrekke K, Mehl S, Nakken O, Pennington M (2001) A survey-based assessment of the northeast Arctic cod stock. *ICES J Mar Sci* 58(4):763–769.

Supporting Information

Eikeset et al. 10.1073/pnas.1525749113

Our model is presented in detail in ref. 27. *S1. Model Description* provides a broad overview and describes model aspects that are of particular relevance to this study. Our model's parameterization is detailed in *S2. Model Parameterization*, the ranking of differently parameterized models is explained in *S3. Model Selection*, an alternative maturation model is examined in *S4. Alternative Maturation Model*, and the population-level dynamics of the four evolving life history traits are shown in *S5. Evolving Traits*. *S6. Comparison with Other Observed Trends* and *S7. Higher Genetic Variances* provide supplementary results on how our model predictions match other observed trends and on how they change for higher levels of genetic variation, respectively. *S8. Model Limitations* discusses key model limitations.

S1. Model Description

Model Overview. We use an individual-based model that follows the evolution of four key life history traits: somatic growth capacity, two traits describing the probabilistic maturation reaction norm (PMRN), and reproductive investment (27): by combining quantitative genetics with ecological processes at the individual level, we derive knowledge on how individuals adapt to the selection pressure from fishing mortality, and thereby affect the fish stock at the population level. Each genetic trait has a heritability that allows us to calculate the environmental variance in the initial population, and this environmental variance is kept constant through time. The genetic traits are assumed to be normally distributed with mean initial trait values and genetic variances determined by the coefficient of genetic variation (CV) in the initial population. The traits are expressed phenotypically by random draws from a normal distribution with means equal to the respective genetic trait (see Table S2 for initial values) and with the corresponding environmental variances. Offspring inherited genetic trait values from their parents by drawing randomly from normal distributions with means equal to the midparental value and variances equal to one-half of the genetic variance of the considered trait in the initial population. After the first year in the simulation, the genetic means, heritabilities, and trait distributions could change freely as determined by the processes of maturation, somatic growth, reproduction, and natural and fishing mortality. These processes were applied sequentially in each year to all individuals.

The genetic growth capacity g_G specifies the maximum growth potential of an individual, which would be realized in the absence of density dependence, that is, when population biomass equals 0. The genetic PMRN intercept i_G and slope s_G affect how an immature individual's probability to mature p_m changes as a function of its age a and length l and is given by $p_m = [1+\exp(-(l-l_{p50,a})/v)]^{-1}$. The length $l_{p50,a}$ is where the maturation probability p_m is equal to 50% at age a, as given by $l_{p50,a} = i_P + s_P a$, with a phenotypic intercept i_P and slope s_P. The parameter v is determined by the lower bound probability p_u (25%) and the upper bound probability p_l (75%) of the maturation envelope, together with the PMRN width w, as given by $v = w/\ln((p_l^{-1}-1)/(p_u^{-1}-1))$. For more information, see ref. 27 and references therein.

Reproductive investment is measured in terms of the gonadosomatic index GSI_G, defined as the ratio of gonadic mass to somatic mass. The phenotypic gonadosomatic index GSI_P and the conversion factor, γ (needed to account for the higher energy content of gonadic tissue relative to somatic tissue), determine the length of a mature individual. A female's fecundity f is given by the individual's length l and gonadosomatic index phenotype GSI_P, $f = kl^j GSI_P D$, where D is the weight-specific packing density of oocytes, and k and j are allometric constants relating body length to body mass.

Our model does not account for pleiotropy or genetic linkage between the traits because the genetic traits evolve independently. Sex is assigned randomly at birth, assuming a 1:1 primary sex ratio. Females and males are otherwise identical and treated equally, with their mating success assumed to be proportional to their gonad mass. Mating is random with replacement, allowing individuals to mate with several different partners, as assumed for batch spawners like Atlantic cod (77, 83). As described in detail in ref. 27, there is a cost to evolving fast growth, implemented through a trade-off between g_G and survival; the derivation of the parameter g_{max} describing this trade-off is discussed below (*S2. Model Parameterization*).

Natural mortality (for the modeling of fishing mortality, see below) originates from newborn mortality, the cost of growth, and a constant background natural mortality. The density-dependent newborn mortality is determined by an estimated Beverton–Holt stock–recruitment relationship, depending on the spawning stock biomass and a climatic variable, sea surface temperature. The number of newborn recruits is then calculated by backcalculating the predicted number of 3-y-olds, assuming an annual total natural mortality rate of 0.2 y^{-1} as assumed by the International Council for the Exploration of the Sea (ICES) in its virtual population analyses (VPAs) (84). The survival probability of the newborn offspring of a spawning pair equals the number of newborn recruits divided by the total fecundity of the spawning population. The modeled growth–survival trade-off describes the reduction in the amount of energy available for maintenance and survival as growth is increased (*S2. Model Parameterization*; ref. 22). Together, the background natural mortality and the additional mortality resulting from the growth–survival trade-off yield natural mortalities equal to ∼0.2 y^{-1} (84).

An important feature of our model is that evolution can be switched on or off according to different model variants (22–24, 43). Evolution can take place only when genetic variation is present: high genetic variation allows for faster evolutionary responses, whereas low genetic variation constrains the pace of evolution (22). We vary the evolvability of each trait in terms of its CV (given by the ratio of genetic SD and genetic mean) in the initial population. We run our model for alternative combinations of the CVs of the four evolving life history traits, thereby manipulating their evolvability, to assess the amounts of evolution required to provide a good match with the observed maturation trends.

In addition to the genetic variances, our model is parameterized from empirical data available for NEA cod, including those representing the initial mean life history trait values, annual fishing mortalities (Fig. S1*A*), the stock–recruitment relationship, and the density-dependent growth relationship (Fig. S1*B*). After the model is initialized, emergent properties arise that include the trait genotypes and phenotypes, as well as stock abundance and biomass.

Density-Dependent Growth. To account for the density dependence of growth, an individual's phenotypic length increment $g_{P,D,t}$ in year t is assumed to be a decreasing function of the total stock biomass $B_{3+,t}$ of individuals aged 3 y and older in year t. We estimated two density-dependent growth models based on available data. The first uses annual mean lengths at age of juvenile cod captured during the Barents Sea winter survey from 1978 to 2009 (84) to estimate annual length increments; we describe this model as representing the "contemporary" time period. Representative

length data characterizing juvenile growth are not available before 1978, and we therefore estimated a second growth model using an alternative source of data collected for a different range of years. Covering the period 1931–1950, we calculated the mean annual growth increment as length at first spawning divided by age at first spawning; we refer to this period as the "historical" time period. The latter method assumes linear growth before maturation (in agreement with observations; ref. 74) and that age at first spawning is accurately estimated (not rigorously validated, but showing only small changes over time and variability among age readers; ref. 36). By construction, it underestimates interannual variation in growth, because the growth until maturation is equally attributed to all juvenile ages. For both growth models and associated time periods, the annual estimates of total stock biomass for ages 3 y and older are based on stock assessment modeling conducted by the Norwegian Institute of Marine Research (IMR) and the ICES (84, 85).

Because the time series for the period 1931–2005 does not have truly annual temporal resolution (as explained above) and does not suggest any statistically significant deviation from linearity, density-dependent growth for the historical period 1931–1950 was estimated using the simplest possible statistical model across years t:

$$g_t = g_0 - bB_{3+,t}, \qquad \textbf{[S1a]}$$

where g_t is the observed mean length increment in the population in year t; g_0 is the intercept, describing mean growth in the absence of density dependence; and b is the slope coefficient, describing the strength of density dependence. In our individual-based model, g_0 thus corresponds to an individual's maximum phenotypic growth capacity $g_{P,t}$ (determined by its genetic growth capacity g_G in conjunction with environmental variation not related to density) and g_t to its realized phenotypic length increment $g_{P,D,t}$ after accounting for density dependence. The endpoint of the historical period was chosen so as to provide enough data for the estimation, while maintaining a clear temporal separation between the historical and contemporary periods; the exact year is arbitrary.

The data for the contemporary time period are of higher quality and allow controlling for several key environmental variables, as well as comparison of different functional forms (linear versus exponential). On this basis, density-dependent growth for the contemporary time period 1978–2009 was estimated through the following statistical model across years t:

$$g_t = g_0^* \exp\left(b^* B_{3+,t}\right). \qquad \textbf{[S1b]}$$

The parameters g_0^* and b^* were estimated by regressing log-transformed mean annual growth increments for ages 0–5 y in the winter survey on total cod biomasses $B_{3+,t}$ (84), annual values of the station-based winter North Atlantic Oscillation (NAO) index (https://climatedataguide.ucar.edu/climate-data/hurrell-north-atlantic-oscillation-nao-index-station-based), mean annual water temperatures from the Kola Section (0- to 200-m depth; courtesy of the Polar Research Institute of Marine Fisheries and Oceanography in Murmansk, Russia), and log-transformed capelin abundances (84). To parameterize Eq. **S1b**, we used the Akaike information criterion (AIC) (86) to select the best model among candidate models including all explanatory variables and their second-order interactions. The best model turned out to include all four explanatory variables and the interactions between capelin abundance and water temperature, water temperature and NAO, and total cod biomass and NAO. The parameter g_0^* was then obtained for the mean environmental conditions, by setting the NAO index to zero and capelin abundance and water temperature to their observed means (2.5×10^9 kg and 4.1 °C, respectively).

The goodness of fit for the historical and contemporary growth models is R^2 = 1.6% and 73%, respectively. Hence, the contemporary growth model provides a good fit with the data, whereas the historical growth model does not. Furthermore, when both models are applied over the full range of biomass levels observed during 1932–2005, the contemporary growth model predicts growth at high biomass levels that is in good agreement with observations from the historical period, whereas the historical growth model fails to provide a good fit with growth at low biomass levels (Fig. S1*B*).

Fishing Mortality. In our model, fishing occurs separately in the feeding grounds and spawning grounds. For the feeding grounds, fishing is size selective with minimum-size limits within the range recorded for NEA cod from the 1980s onward (87). For the spawning grounds, only mature individuals are fished and no minimum-size limit is applied. To mimic the historical fishing pressures, we use estimates of the annual fishing probabilities from the feeding grounds and spawning grounds covering the period 1932–2005 (data provided by the IMR). These estimates are obtained using a method that relies on the Baranov catch equation, canonically assuming a natural mortality rate of 0.2 y^{-1}. This method takes as inputs the maturity ogive, the estimated numbers of fish in the population and in the catch per age and year (available from the stock assessment; refs. 84 and 85), and the estimated numbers of fish caught on the spawning grounds (ref. 32 and official Norwegian catch statistics). The resultant age-specific estimates of the annual fishing probabilities are geometrically averaged over the ages from 5 to 12 y (for the feeding grounds, with the lower age corresponding to the age of full recruitment to the fishery) or over the ages from 7 to 12 y (for the spawning grounds). To account for the time spent by mature fish on the spawning grounds, for an assumed annual duration of 3 mo or one-quarter of the year, the fishing probability of mature fish on the feeding grounds is given by $1-(1-p_0)^{3/4}$, where p_0 is the annual fishing probability of immature fish on the feeding grounds. A constant mean fishing mortality rate was estimated and applied for the years before 1932, to represent the earliest period of fishing (31).

S2. Model Parameterization

Parameter values for our model (Table S2) are based on published sources, data collected by the IMR, and survey data made available through the ICES. For further details, see ref. 27.

As reported above and in further detail in ref. 27, we used a model-fitting exercise to fine-tune the strength of the trade-off between growth and survival, measured by the parameter g_{max}, for which directly applicable data are unavailable. Model fitting has recurrently been used to derive unknown parameter values for stock assessment models. To do this, we "precalibrated" the nonevolutionary model to match stock dynamics during the period 1932–1950. Specifically, log-likelihood (*S3. Model Selection*) was used to select the value of g_{max} that maximizes the fit between model predictions and observed data on the age and length at maturation and phenotypic growth. The tested values of g_{max} (50–200 cm in increments of 5 cm) cover those assumed in previously published versions of our model (22, 73).

Observed stock abundances and biomasses are scaled down by a factor of 100,000 to obtain a computationally feasible number of individuals to track in our model (~50,000). The model describes each individual's growth, maturation, reproduction, and mortality. Accordingly, the model parameters describing the density dependences of recruitment and growth are divided by this scaling factor. Likewise, for presenting results, the modeled stock abundances and biomasses are multiplied by the same factor (100,000) to scale them up to the observed values, and thus

recreate the realistic stock levels. This scaling does not affect the stock's ecological and evolutionary dynamics and simply means that the tracked individuals in the scaled-down model can be interpreted as superindividuals (88, 89).

We vary the CVs of all four considered life history traits to determine the amounts of evolution needed to match the maturation trends for 1932–2005 (*S3. Model Selection*). Evolving populations with different CVs share the same mean genetic trait values in 1932. For some combinations of CVs, the applied fishing mortalities cause stock extinction, defined as occurring when stock abundance fall below 20 mature superindividuals; these combinations are excluded from further analysis.

S3. Model Selection

Allowing each of the considered four life history traits to have a CV that is either zero or positive results in $2^4 = 16$ different model variants.

Assuming that the observed variables—average year-specific ages and lengths at maturation, that is, average year-specific ages and lengths of first-time spawning fish—follow normal distributions with means specified by the model variant and the associated four CVs, $CV = (CV_g, CV_i, CV_s, CV_{GSI})$, and denoting the observed average age and length at maturation in year t by a_t and l_t, respectively, the corresponding model predictions by $\tilde{a}_t(CV)$ and $\tilde{l}_t(CV)$, respectively, and the corresponding variances of the aforementioned normal distributions by σ_a^2 and σ_l^2, a model variant's likelihood given the observations (a_t, l_t) for $t = t_{min}, \ldots, t_{max}$ is as follows:

$$L(CV, \sigma_a^2, \sigma_l^2) = \prod_{t=t_{min}}^{t_{max}} \frac{1}{\sqrt{2\pi}\sigma_a/u_a} \exp\left(-\frac{1}{2\sigma_a^2}\left(a_t - \tilde{a}_t(CV)\right)^2\right) \times \prod_{t=t_{min}}^{t_{max}} \frac{1}{\sqrt{2\pi}\sigma_l/u_l} \exp\left(-\frac{1}{2\sigma_l^2}\left(l_t - \tilde{l}_t(CV)\right)^2\right), \quad \textbf{[S2a]}$$

where $t_{min} = 1932$ and $t_{max} = 2005$ are the years at the beginning and end of the comparison period, which has a duration of $T = t_{max} - t_{min} + 1 = 74$ y. As the likelihoods resulting for the 16 model variants span several orders of magnitude, we follow the custom of reporting log-likelihoods, $\ln L$. The unit-standardizing constants $u_a = 1$ y and $u_l = 1$ cm make likelihoods and log-likelihoods dimensionless, and thereby ensure that all terms contributing to the log-likelihood function are dimensionally commensurable. Although they affect the log-likelihood values reported in Table 1, they have no bearing on likelihood ratios and log-likelihood differences, and therefore do not influence the ranking of model variants.

The unknown variances σ_a^2 and σ_l^2 are estimated so as to have maximum likelihood (e.g., ref. 90, pp. 354–355):

$$\sigma_a^2(CV) = \frac{1}{T}\sum_{t=t_{min}}^{t_{max}} \left(a_t - \tilde{a}_t(CV)\right)^2,\ \sigma_l^2(CV) = \frac{1}{T}\sum_{t=t_{min}}^{t_{max}} \left(l_t - \tilde{l}_t(CV)\right)^2. \quad \textbf{[S2b]}$$

Substituting Eqs. **S2b** into Eq. **S2a** yields the function $L(CV)$, based on which maximum-likelihood CVs are determined for each model variant. To identify the combination of CVs that maximizes this function, a model variant's positive CVs are systematically and independently varied from 2% to 14% in steps of 2%. The upper bound is chosen based on empirical observations (74, 77) and previous models (22, 23, 73), and the discretization is chosen to ensure computational tractability.

To account for the fact that model variants with a larger number of positive CVs have more flexibility in matching the data (and may therefore be considered inappropriately advantaged when ranked just according to their likelihood), we also assessed model variants according to the Akaike information criterion (AIC):

$$AIC = -2\ln L + 2p, \quad \textbf{[S2c]}$$

where p is a model variant's number of positive CVs.

Table S1 shows the resultant ranking of model variants according to their log-likelihood, together with the corresponding AIC differences. A short version of this table is included in the main text, as Table 1.

S4. Alternative Maturation Model

Motivated by the finding of stock collapse when using the density-dependent growth model for the historical period (1932–2005; Fig. 1 *A* and *B*), we apply our nonevolutionary model to an alternative maturation model, obtained by pooling PMRNs over the cohorts of 1932–2005 (Table S2).

This alternative maturation model predicts higher survival and avoids stock collapse through earlier maturation but, as shown in Fig. S2, yields only a very poor fit with the empirical maturation trends (the log-likelihood equals −228.64 and the AIC difference equals 95.5).

S5. Evolving Traits

Fig. S3 shows the population-level changes in the four evolving life history traits predicted by the maximum-likelihood model variants for each of the two density-dependent growth models.

S6. Comparison with Other Observed Trends

Even though the evolvability of traits in our model is calibrated solely based on matching the observed trends in age and length at maturation, our model performs well, for both density-dependent growth models, also with respect to matching the trends in length at age (Fig. S4) and phenotypic growth (Fig. S5*A*). Furthermore, our model succeeds in capturing the trend observed in spawning stock biomass, except for the strong increases in 1935 and 1946 (Fig. S5*C*). In absolute terms, however, our model's match with observed spawning stock biomasses is good only until the 1980s, after which the model fails to predict the pronounced increase in spawning stock biomass observed from 1990 onward (Fig. S5*D*). Our model-predicted total biomass is consistently lower than reported from virtual population analyses by ICES (84, 85). For phenotypic growth, our model performs well throughout the whole time period (Fig. S5*A*). The average number of recruits (at the age of 3 y) is also predicted quite well; however, our model does not capture the four to five substantial pulses in recruitment that gave rise to strong age classes (Fig. S5*B*).

S7. Higher Genetic Variances

To obtain a good fit between model predictions and data on the age and length at maturation, a lower CV in the traits describing the PMRN is needed than what has been assumed in previous models (22, 23, 73). As a result, we observe less evolution of the PMRN than in other modeling studies (22).

In previous eco-genetic models not calibrated for specific stocks, the CVs were assumed to equal 8% (22, 73) or 6% (23). To compare our results to these previous models, we ran our model with CVs in all traits set to either 8%, as considered by Dunlop et al. (22, 73), or 14%, the maximum value in our search grid. Results for both density-dependent growth models are shown in Fig. S6. These results support our main findings in Table 1, which suggest that the CVs do not have to be as large as 8% to match data on maturation. When using CVs equal to 8%, we predict higher rates of PMRN evolution, which are closer to the predictions by Dunlop et al. (22). For NEA cod, values lower than 8% or 6% produce superior fits to the data for this particular stock and for this particular set of conditions.

When interpreting these results, it is important to reflect on how our model accounts for the probabilistic nature of maturation. An individual's maturation occurs randomly according to age- and length-dependent probabilities described by its PMRN. The span between this function's 25% and 75% contours is known as the PMRN width, which at the individual level in our model is kept nonevolving and independent of age. A population's PMRN is given by averaging the PMRNs of all its individuals. We thus initialize our model by assigning individual-level PMRNs so that their average intercepts, their average slopes, and their widths match those of the empirically estimated population-level PMRN for 1932. The genetic variances in PMRN intercepts and slopes that we implement in the model for the initial population introduce variation around the population's mean PMRN intercept and slope and thereby widen the realized population-level PMRN width as the CVs of PMRN intercept and slope are increased. For small CVs, this effect is negligible, whereas, for larger CVs, the realized population-level PMRN width in the model begins to exceed the empirically estimated population-level PMRN width. As a consequence, the model-predicted mean age at maturation in 1932 underestimates the observed value by about 1 y, as seen in Fig. 1 (although the subsequent trends through time are better predicted). As seen in Fig. S6, when the PMRN CVs are as large as 14%, the underestimation of the initial age at maturation increases to 2 y. It then also causes an underestimation of the initial length at maturation by about 15 cm. The effect thus penalizes models with larger CVs in our model selection, leading to larger differences, already in 1932 and then also beyond, between model predictions and observations as the two PMRN CVs are made larger.

It is uncertain what the true PMRN CVs are, which is one of our motivations for running scenarios for many possible combinations of CVs and letting the data "decide" which combinations have the most support. The PMRN width is a poorly studied trait, with potential evolutionary dynamics we do not yet sufficiently understand. An interesting challenge for future research would be to explore PMRN-width dynamics further and to examine whether model variants with higher CVs receive better support when the effect described in the previous paragraph is removed. One approach for doing this would be to reduce the widths assigned to individual-level PMRNs when increasing the PMRN CVs, so as to keep the initial population-level PMRN width in the model in agreement with the corresponding empirically estimated population-level PMRN width. However, such an adjustment is not expected to change two of the main conclusions of our study that (*i*) evolution is required to prevent stock collapse and (*ii*) phenotypic plasticity can partly account for the observed maturation trends when growth is strongly density dependent.

S8. Model Limitations

General model limitations and simplifying assumptions are discussed in Dunlop et al. (22), where also a sensitivity analysis of several model parameters can be found. It is worth pointing out again here that, although we model multitrait evolution, we do not input any explicit genetic correlations between traits. This choice is motivated by the lack of data on genetic covariances between traits in wild stocks of Atlantic cod and by our preference to keep the model's parameterization as simple as possible given the already high complexity of other parts of the model. The effects of trait covariances would be worth investigating in future research.

As mentioned in *S7. Higher Genetic Variances*, our model predictions are close to empirical observations for maturation in the initial simulation year (1932) when the CVs for the PMRN intercept and slope are low, but not when they are high. A better correspondence in the initial year could be achieved by reducing individual-level PMRN widths in accordance with the CVs assumed for the PMRN intercept and slope, which we therefore highlight as an opportunity for future research.

As mentioned in *S6. Comparison with Other Observed Trends*, compared with estimates from the ICES stock assessment models (91) our model-predicted total biomass is consistently lower and our model-predicted spawning stock biomass does not increase toward the end of the time series (Fig. S5). There are several possible explanations for these discrepancies, some relating to our model assumptions and others to potential issues with the biomass data in the stock assessment model. First, we use a constant minimum-size limit for fishing in the feeding grounds, whereas in reality size selectivity has varied. Second, we do not include interactions with other species or effects of environmental change, which could influence biomass through effects on growth and recruitment (92). Third, the population's length–weight relationship might not be constant through time as assumed in our model (75, 77). Fourth, the biomass estimates from ICES are model-based estimations from virtual population analyses and are therefore subject to their own set of assumptions: parts of this discrepancy might be due to uncertainty attached to those estimates (93). Despite the biomass discrepancy, the model-predicted lengths at age match historical data well, especially for the contemporary density-dependent growth model (Fig. S4).

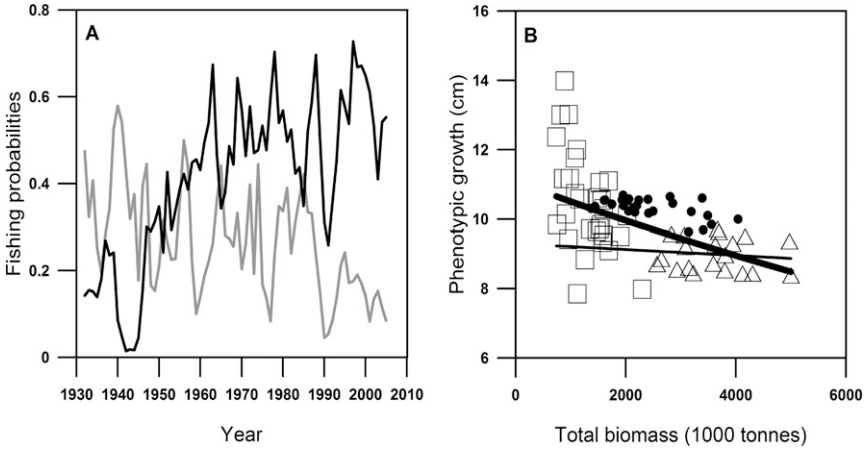

Fig. S1. Time-dependent fishing mortality and density-dependent growth. (*A*) Annual fishing probabilities in the spawning grounds (gray line) and feeding grounds (black line) between 1932 and 2005. (*B*) Mean annual length increments between 1932 and 2005 depending on the total biomass of individuals aged 3 y and older as obtained from virtual population analysis for NEA cod. The density dependence of growth appears to have changed over time, from being weak in the historical period from 1932 to 1950 (triangles) to getting stronger in the contemporary period from 1978 to 2009 (squares). We separately estimated this dependence for both time periods, resulting in what we refer to as the "historical growth model" and the "contemporary growth model." The fitted regression models are shown over the full range of biomasses from 1932 to 2005 for the historical (thin line) and contemporary (thick line) density-dependent growth model. Data for the intermediate period from 1951 to 1977 are shown as black circles.

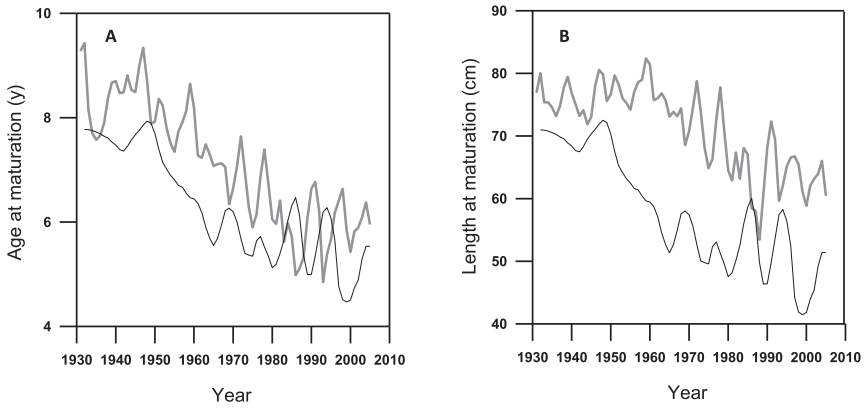

Fig. S2. Test of the alternative maturation model. Like Fig. 1, the figure shows a comparison of model predictions (black lines) and observed data (gray lines) on (*A*) age and (*B*) length at maturation in NEA cod; here, the model predictions are based on a nonevolutionary model using an alternative probabilistic maturation reaction norm (PMRN) estimated by pooling the PMRNs for cohorts from 1932 to 2005. Model predictions are the mean age and length at maturation among individuals in the population, averaged over 30 independent model runs.

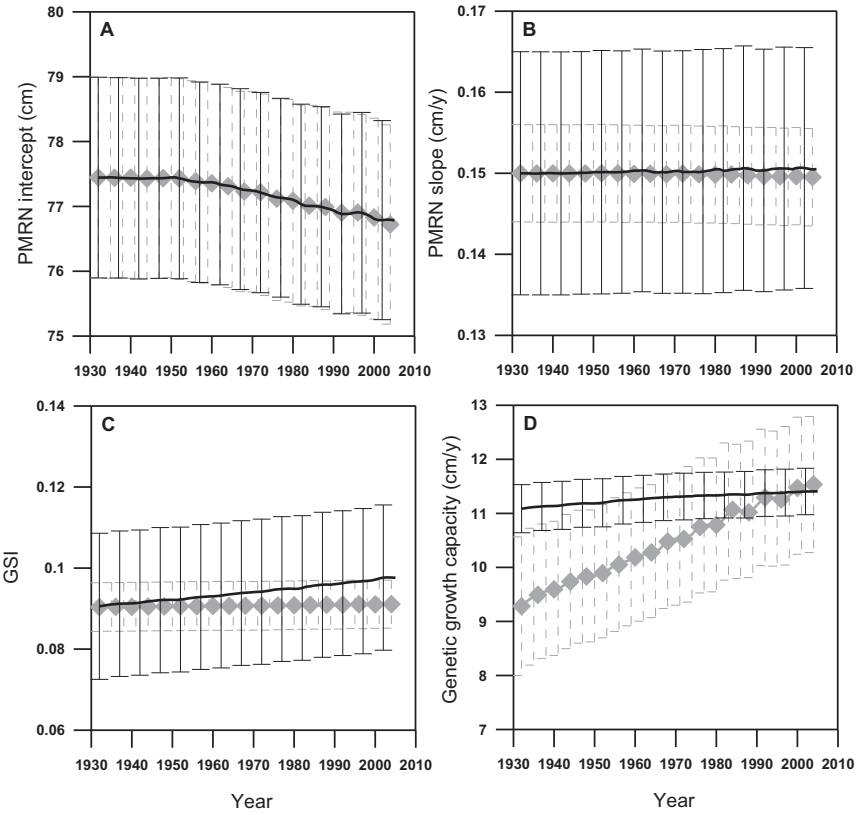

Fig. S3. Population-level changes in the four evolving life history traits. (*A*) Probabilistic maturation reaction norm (PMRN) intercept, (*B*) PMRN slope, (*C*) gonadosomatic index (GSI), and (*D*) genetic growth capacity. Predictions are based on the two maximum-likelihood model variants for the historical (gray) and contemporary (black) growth model, respectively. Points show means among individuals in the population, averaged over 30 independent model runs. Error bars show SDs, averaged over model runs, of individual-level trait values.

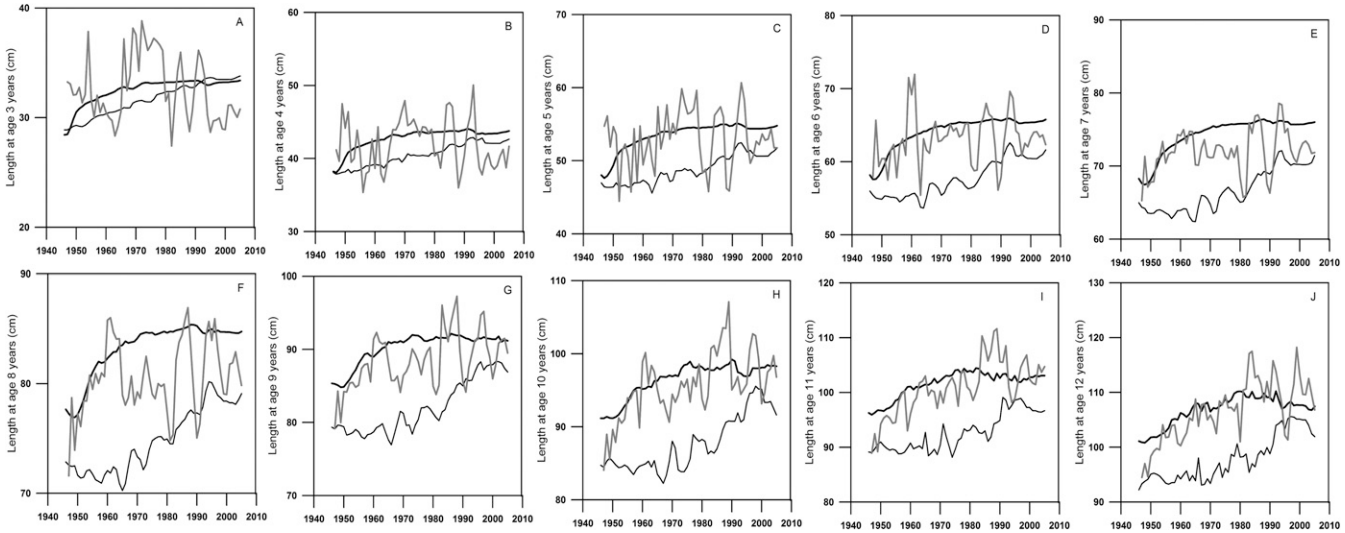

Fig. S4. (*A–J*) Changes in lengths at age across ages 3–12 y. For the years 1946–2004, empirical data (gray lines) are compared with model predictions based on the maximum-likelihood model variants for the historical (thin black lines) and contemporary (thick black lines) growth models. Model predictions show means among individuals in the population, averaged over 30 independent model runs. The shown empirical data were kindly provided by C. T. Marshall, University of Aberdeen, Aberdeen, Scotland.

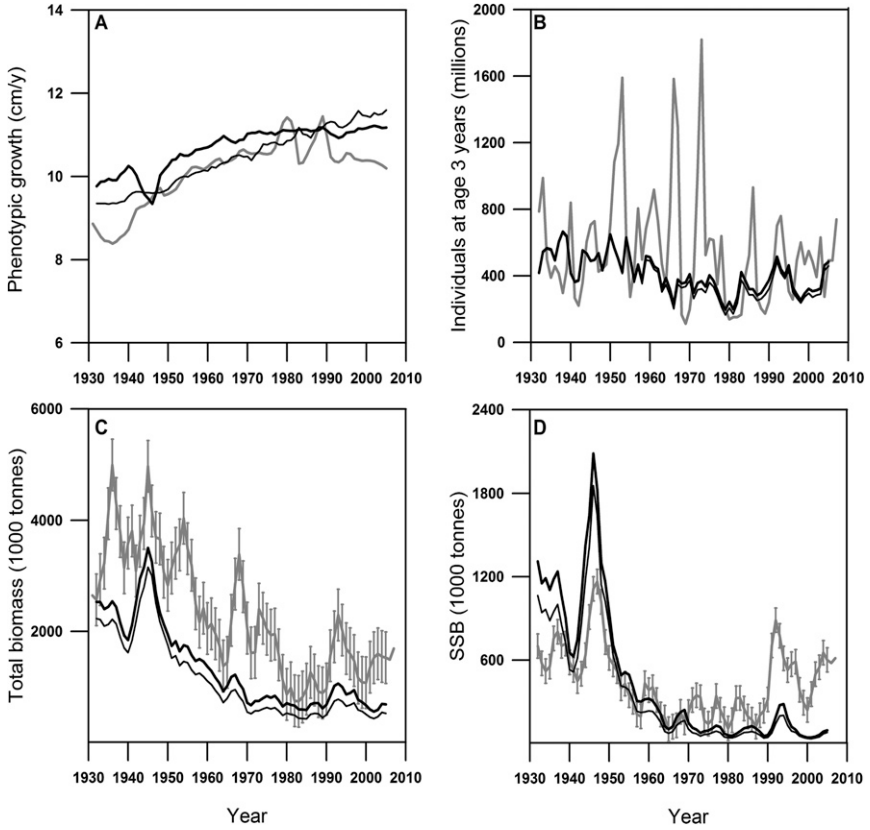

Fig. S5. Changes in emergent life history traits. For the years 1932–2005, empirical data (gray lines) are compared with model predictions based on the maximum-likelihood model variants for the historical (thin black lines) and contemporary (thick black lines) growth models. (*A*) Mean annual length increments, (*B*) number of recruits at the age of 3 y, (*C*) total biomass of individuals aged 3 y and older, and (*D*) spawning stock biomass. For illustration, error bars in *C* and *D* show the span of values corresponding to a coefficient of variation of 20%, which is roughly indicative of the assumed estimation error. Model predictions show means among individuals in the population, averaged over 30 independent model runs.

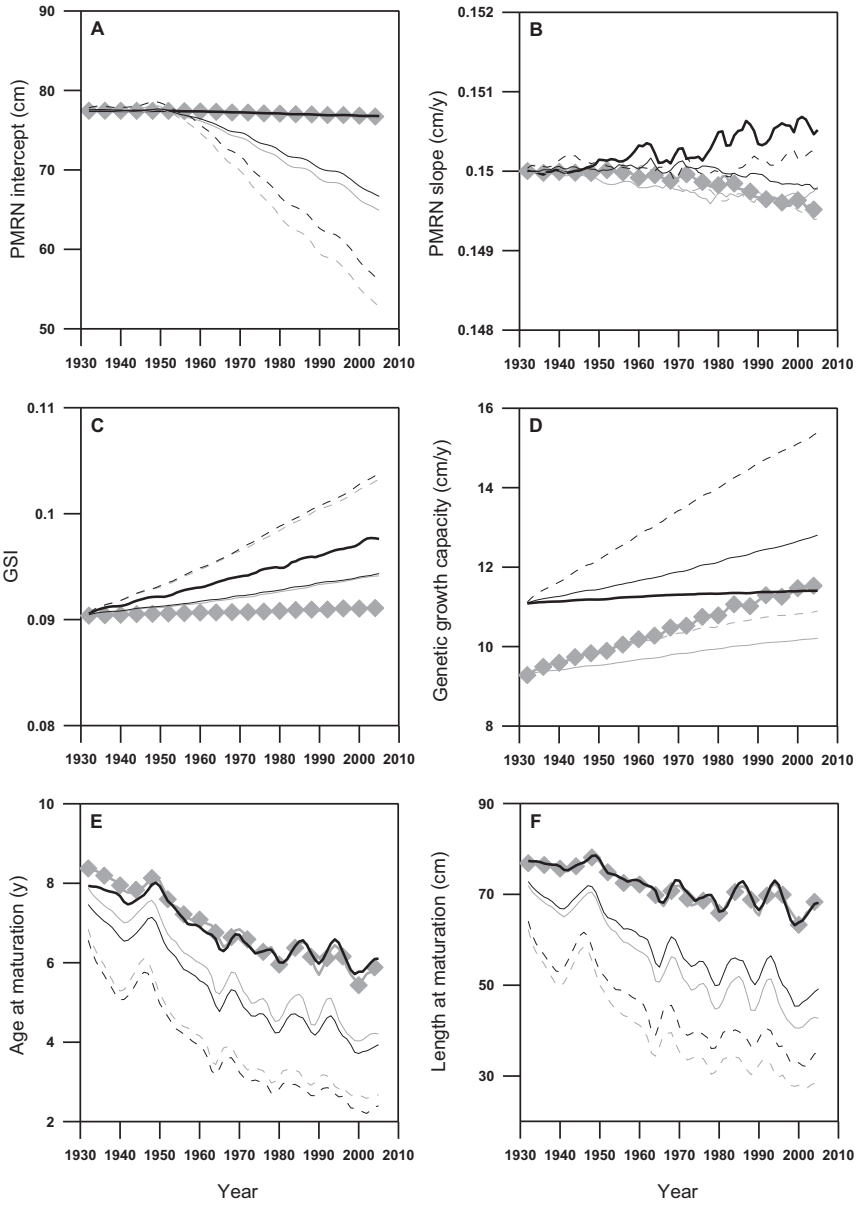

Fig. S6. Test of higher genetic variances. (*A*) Probabilistic maturation reaction norm (PMRN) intercept, (*B*) PMRN slope, (*C*) gonadosomatic index (GSI), (*D*) genetic growth capacity, (*E*) age at maturation, and (*F*) length at maturation. The maximum-likelihood model variants for the historical (thick gray lines with diamond markers) and contemporary (thick black lines) growth models are compared with model variants in which all CVs are set to 8% (thin continuous lines) or 14% (thin dashed lines). Model predictions show means among individuals in the population, averaged over 30 independent model runs.

Table S1. Top-ranked model variants with their CVs for the four considered life history traits (g, growth capacity; GSI, gonadosomatic index; i, PMRN intercept; s, PMRN slope)

CV					
CV_i	CV_s	CV_g	CV_{GSI}	Log-likelihood, ln L	AIC difference
i) Historical density-dependent growth model for 1932–1950*					
0.02	**0.06**	**0.14**	**0.02**	**−177.74**†	1.7
0.02	*0*	*0.14*	*0.08*	−177.88	*0*
0.02	0.02	0.14	0	−178.14	0.5
0	0.12	0.14	0.02	−178.79	1.8
0.02	0	0.14	0	−179.33	0.9
0	0	0.14	0.02	−180.30	2.8
0	0.02	0.14	0	−180.45	3.1
0	0	0.14	0	−181.50	3.2
ii) Contemporary density-dependent growth model for 1978–2009					
0.02	**0.1**	**0.04**	**0.12**	**−181.22**†	2.9
0.02	0.02	0	0.06	−181.74	2.0
0.02	0.04	0	0	−181.78	0.1
0.02	0	0.04	0	−181.80	0.1
0.02	0.14	0.04	0	−181.82	2.1
0.02	0	0.04	0.08	−181.86	2.2
0.02	0	0	0.1	−181.94	0.4
0	0.14	0.04	0.14	−182.29	3.1
0.02	*0*	*0*	*0*	−182.75	*0*
0	0	0.04	0.04	−183.05	2.6
0	0	0	0.04	−183.09	0.7
0	0	0.04	0	−183.19	0.9
0	0.02	0	0.04	−183.38	3.3
0	0.14	0.02	0	−183.46	3.4
0	0.04	0	0	−183.80	2.1
0	0	0	0	−184.04	0.6

Two alternative density-dependent growth models are considered: (*i*) the historical growth model estimated from data available for 1932–2005 and (*ii*) the contemporary growth model estimated from data available for 1978–2009. For each growth model, we consider the 16 model variants resulting from allowing each of the four traits to have a CV that is either zero or positive. For each model variant, the positive CVs are chosen to have maximal likelihood on a four-dimensional grid ranging from 0% to 14% in steps of 2%. The nonevolutionary model is defined by all four CVs being set to 0. The models with viable populations are ranked by their log-likelihood ln L (higher is better) and further assessed by their difference in the AIC relative to the model variant with the lowest AIC (lower is better). For each growth model, the best-fitting model variants are highlighted (in bold for the maximum likelihood and in italics for the lowest AIC).

*In the nonevolutionary model with historical density-dependent growth, as well as in the not shown seven evolutionary model variants, the population goes extinct.

†Having maximum likelihoods, these model variants are shown in Fig. 1.

Table S2. Model parameters, values, and sources

Description	Source[†]	Value
Initial mean genetic PMRN[‡] intercept, $\bar{i}_G$	1	77.4 or 69.33[§] cm
Initial mean genetic PMRN[‡] slope, $\bar{s}_G$	1	0.15 or 0.99[§] cm·y^{-1}
Initial mean genetic PMRN[‡] width, $\bar{w}_G$	1	12.88 or 15.76[§] cm
Initial mean genetic growth capacity, $\bar{g}_G = g_0$[¶]	2	9.3 cm
Initial mean genetic growth capacity, $\bar{g}_G = g_0^*$[#]	2	11.08 cm
Parameter in density-dependent growth model, b[¶]	2	$-8.57\ 10^{-6}$ cm·kg^{-1}
Parameter in density-dependent growth model, b^*[#]	2	$-5.34\ 10^{-6}$ kg^{-1}
Initial mean genetic reproductive investment, $\overline{GSI}_G$	3	0.09
Reproductive investment conversion factor, γ	4	0.60241
Spawning-ground harvest probability before 1932	5	0.38
Immature feeding-ground harvest probability before 1932	5	0.09
Minimum-size limit on feeding grounds	6	45 cm

[†]Sources: 1, ref. 21 and M.H., O. R. Godø, and U.D. (IMR data); 2, IMR survey data for NEA cod from 1932 to 2005 (provided by M.H. [Institute of Marine Research (IMR), Bergen, Norway; University of Bergen, Bergen, Norway; and International Institute for Applied Systems Analysis (IIASA), Laxenburg, Austria], O. R. Godø (Institute of Marine Research, Bergen, Norway), and U.D. (International Institute for Applied Systems Analysis, Laxenburg, Austria) from IMR data); 3, ref. 2; 4, refs. 11 and 12; 5, ref. 22 and M.H., O. R. Godø, and U.D. (IMR data); 6, ref. 13.
[‡]PMRN, probabilistic maturation reaction norm.
[§]PMRN estimated for cohorts pooled from 1932 to 2005.
[¶]Historical growth model estimated for 1932–1950 (Eq. **S1a**).
[#]Contemporary growth model estimated for 1978–2009 (Eq. **S1b**).